

GlowGS: Generative Semantic Feature Learning for 3D Gaussian Splatting in Nighttime Glow Scenes

Beibei Lin Xiao Cao Jingyuan Guo Robby T. Tan
National University of Singapore

beibei.lin@u.nus.edu, robbly.tan@nus.edu.sg

Abstract

Existing 3DGS methods effectively render high-quality novel views in clear-day scenes. However, they struggle with night scenes, particularly in glow regions, due to the lack of structural features such as textures and edges, which are key cues for splatting-based reconstruction. To address this problem, we leverage a diffusion model and a Vision Foundation Model (VFM) to compensate for missing structural cues. Our method consists of two key novel ideas: semantic feature generation and novel-view semantic learning. First, semantic feature generation produces high-quality semantic features as implicit structural cues for novel views. Specifically, a diffusion model synthesizes novel views with unknown camera poses from training views, while a VFM evaluates their quality. Once high-quality novel views are identified, the VFM extracts robust features to construct the semantic feature bank. Second, novel-view semantic learning enables 3DGS to optimize rendered novel views without requiring ground truth. It achieves this by extracting semantic features from a rendered novel view, searching the feature bank for the most similar features, and minimizing their distance. This process enforces implicit structural constraints, ensuring semantically coherent, artifact-free rendered views. Extensive experiments demonstrate the effectiveness of our GlowGS in generating semantically accurate 3D views, showing significant improvements over existing methods.

1. Introduction

Existing 3D Gaussian Splatting (3DGS) methods (e.g., [26, 29, 64]) demonstrate strong performance in rendering novel views of clear-day scenes but struggle with complex nighttime scenes, particularly in glow regions that lack distinct structural features [21, 36]. These regions exhibit intensity and color variations without physical surfaces, preventing 3DGS from capturing reliable geometric structures. While 3DGS effectively models these areas in training views, it

fails to generalize, leading to artifacts in novel view synthesis. As shown in Figure 1, existing 3DGS methods perform poorly in glow regions.

In this paper, we introduce **GlowGS**, a nighttime 3DGS method for rendering novel views of night scenes with prominent glow regions. GlowGS is built on two key components: semantic feature generation and novel-view semantic learning. Our semantic feature generation employs a diffusion model and a Vision Foundation Model (VFM), such as DINO [3] and CLIP [48], to produce high-quality semantic features, providing implicit structural cues for novel views. As shown in Figure 6, the VFM effectively generates discriminative representations in glow regions. We use an image-to-video diffusion model, such as Pika [46] or PromeAI [47], to synthesize novel views with unknown camera poses from training images, enabling the capture of multi-view glow information.

However, the generation process may introduce inaccuracies and artifacts. To address this, we use a VFM-based verification process to assess the quality of generated novel views. The VFM extracts features from both training and generated views, measures their similarity, and selects high-quality novel views accordingly. Once identified, it extracts robust features to construct the semantic feature bank. Since these features are extracted from generated views with unknown camera poses, they cannot be directly used for novel view training. To overcome this, we introduce novel-view semantic learning, enabling 3DGS to optimize novel views using the semantic feature bank. This approach builds on the idea that similar regions share closely related semantic features despite minor pixel variations. As a result, the semantic features in our bank constrain corresponding regions in novel views rendered by 3DGS.

Unlike traditional 3DGS, which optimizes only training views, our approach also renders novel views and extracts their semantic features during training. These features are queried against the semantic feature bank, retrieving the most similar ones by minimizing their distance. This process allows 3DGS to progressively refine missing structural information through feature optimization. As shown in Fig-

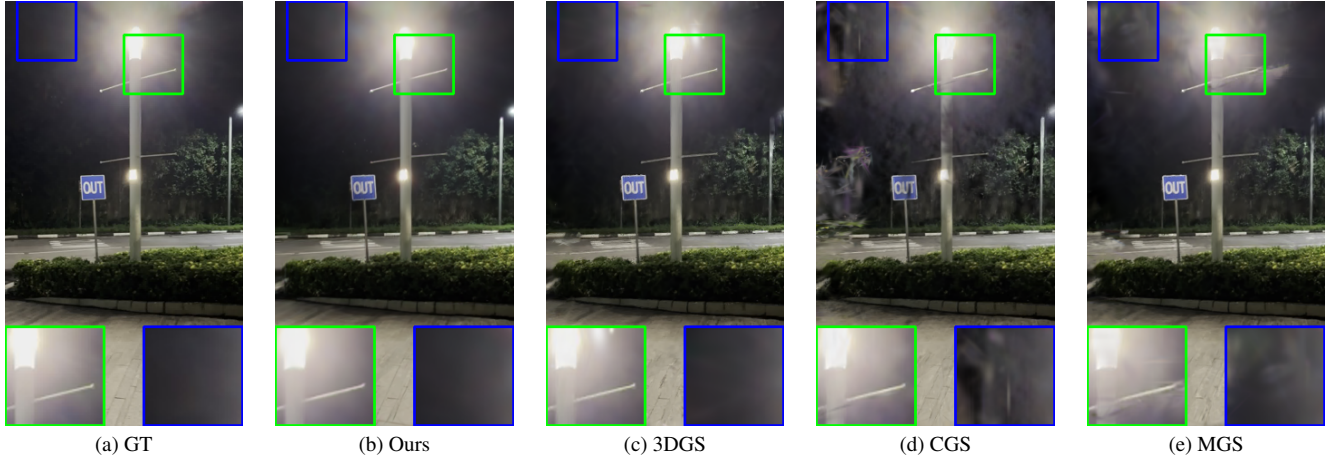


Figure 1. Qualitative results from 3DGS [26], CGS [29], MGS [64], and our method on nighttime scenes. All results are from novel views. The zoom-in insets highlight artifacts in glow regions produced by existing methods, including duplicated light sources and unnatural bright spots in dark areas. Our method reconstructs glow regions with smoother light diffusion, effectively reducing these artifacts.

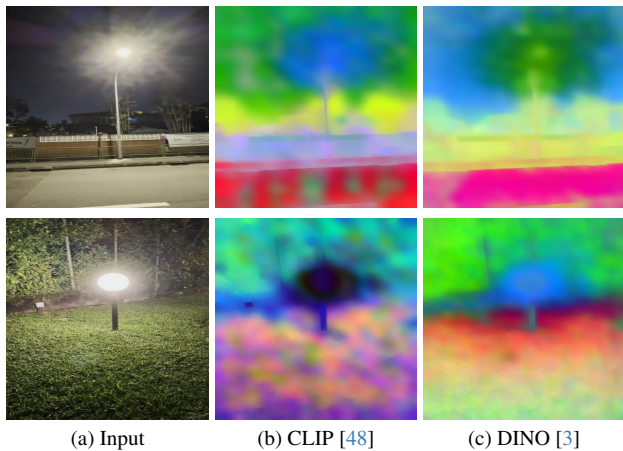


Figure 2. Visualization of features extracted by different Vision Foundation Models.

ure 1, our method effectively reconstructs nighttime scenes, including glow regions.

As no dataset exists for evaluating 3D scene reconstruction in nighttime settings with strong glow, we introduce **NightGlow**, a new dataset for this task. NightGlow consists of 18 scenes with approximately 540 images, all featuring a strong presence of glow. Both qualitative and quantitative results show that GlowGS effectively reconstructs glow regions in novel views. Moreover, GlowGS is model-agnostic, making it compatible with various 3DGS techniques, including 3DGS [26], CGS [29], and MGS [64]. Our key contributions are as follows:

- **Semantic feature generation:** We introduce a method that combines a diffusion model and Vision Foundation Models (VFM) to generate high-quality semantic fea-

tures, providing implicit structural cues for novel views.

- **Novel-view semantic learning:** We propose a learning strategy that enables 3D Gaussian Splatting to optimize novel views without ground-truth supervision, enforcing implicit structural constraints to ensure semantically accurate, artifact-free renders.
- **Extensive experiments:** We conduct comprehensive experiments demonstrating that GlowGS significantly improves the reconstruction of real-world nighttime glow scenes. Our method outperforms MGS [64], achieving a 1.78 improvement in PSNR.

2. Related Work

Novel View Synthesis Given several captured images with corresponding viewpoints, Novel View Synthesis (NVS) generates new images from different viewpoints [17, 30]. Neural Radiance Fields (NeRF)[41] achieves this via volume rendering[38, 39], using MLPs [9, 40, 44] to model scenes as continuous functions, providing a compact representation. However, its rendering speed is slow due to MLP evaluation at each ray point. To enable real-time rendering, some methods distill a pre-trained NeRF into a sparse representation [19, 49, 62, 63]. More recently, advanced scene representations have been developed to boost training and rendering efficiency [2, 4, 10, 14, 26, 28, 43, 56]. Despite these advancements, NeRF-based methods still face slow rendering speeds, limiting their real-time application.

3D Gaussians Splatting (3DGS) [26, 29, 51, 64] has been proposed for 3D scene reconstruction. Unlike NeRF, which uses MLPs to model scenes as continuous functions, 3DGS represents scenes with Gaussian distributions, enabling efficient rendering by projecting these Gaussians onto 2D views. Lee et al. [29] introduce Compact 3DGS, using a

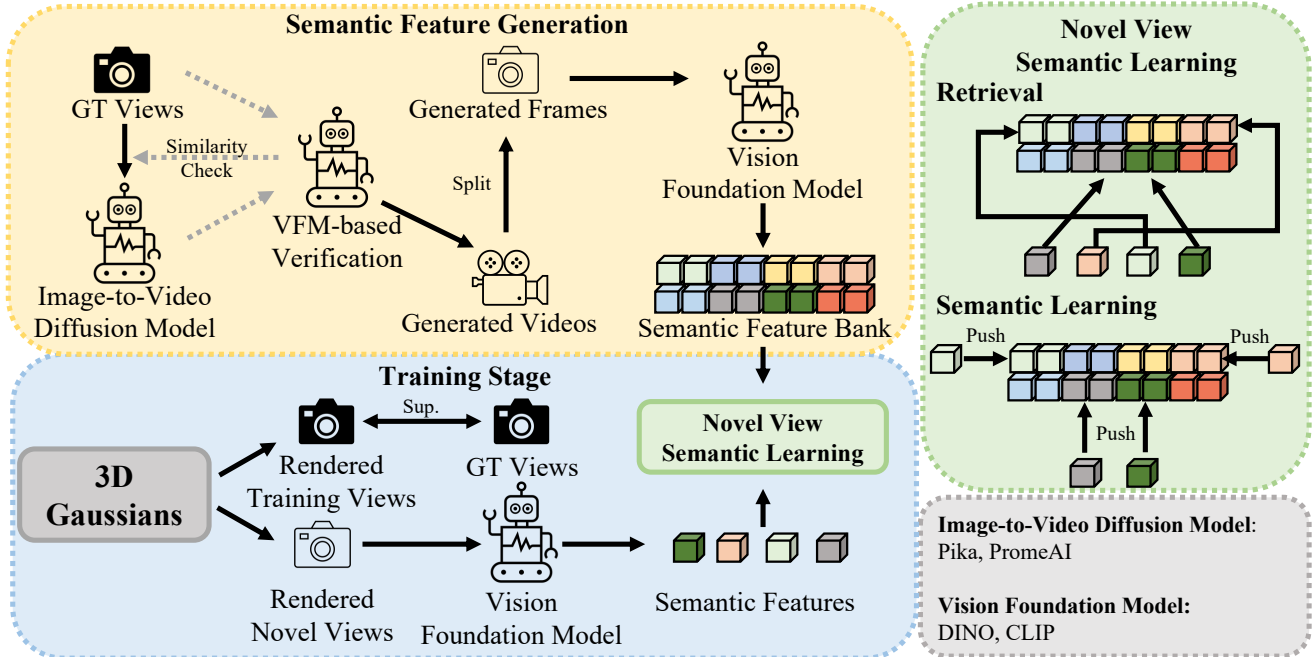


Figure 3. **Overview of our GlowGS, which centers around two core ideas:** semantic feature generation and novel-view semantic learning. Given the training views, our semantic feature generation uses image-to-video diffusion models to create novel views with unknown poses, followed by a VFM-based module to assess their quality. We then extract robust semantic features from the high-quality views and build a semantic feature bank. In novel-view semantic learning, we refine these views by extracting their features, retrieving the most similar ones from the bank, and minimizing the distance between them to ensure consistency and quality.

learnable mask strategy to reduce Gaussians while preserving performance. Yu et al. [64] add a 3D smoothing filter to address artifacts from varying sampling rates and replace the 2D dilation filter with a 2D Mip filter to reduce aliasing and dilation.

Diffusion Models and Vision Foundation Models Existing large-scale pretrained diffusion models [8, 20, 33–35, 37, 45–47, 50, 53, 55] and Vision Foundation Models [3, 18, 27, 48] excel in image and video generation, as well as image understanding. Specifically, [50] introduces a latent-based diffusion model for image generation, while large-scale pretrained models by Pika [46] and PromeAI [47] have shown remarkable video generation capabilities, extending a single video frame into a high-fidelity 4-second clip. Vision foundation models like DINO [3] and CLIP [48] demonstrate advanced image understanding. Trained using self-supervised strategies, they learn from vast amounts of unlabeled data, leading to enhanced image comprehension.

3. Proposed Method: GlowGS

Figure 3 provides an overview of GlowGS, highlighting its two key components: semantic feature generation and novel-view semantic learning. The details are as follows.

3.1. Semantic Feature Generation

Our semantic feature generation, illustrated in the yellow panel in Figure 3, synthesizes novel views with unknown camera poses using an image-to-video diffusion model. It then extracts their semantic features with a Vision Foundation Model (VFM) and stores them in a semantic feature bank. This whole process consists of three core components: image-to-video generation, VFM-based verification, and feature extraction.

Image-to-Video Generation Here, we aim to synthesize novel views with unknown camera poses from the training views of a scene using an image-to-video diffusion model [46, 47]. Given a scene $\mathbf{D} = \{f_i^0 | i = 1, 2, \dots, N\}$, where f_i^0 is the i -th training view and N is the number of training views, the generation is formulated as:

$$\mathbf{V}_i = \mathbf{F}_{\text{I2V}}(f_i^0), \quad (1)$$

where $\mathbf{F}_{\text{I2V}}(\cdot)$ is the image-to-video diffusion model, and $\mathbf{V}_i = \{f_i^j | j = 1, 2, \dots, M\}$ represents the set of M generated novel views.

Since the camera poses for each novel view f_i^j are unknown due to the synthetic and random generation process, they cannot directly guide the training of our 3DGS. The

generated views may also suffer from hallucinations, inconsistencies, and low quality. To address these issues, we introduce a VFM-based verification method to assess the quality of the generated views \mathbf{V}_i .

VFM-based Verification We leverage a VFM, such as DINO [3], to evaluate the quality of the generated videos. Our main idea is that the generated views should closely match the semantic content of the original frame. With its image understanding capabilities, the VFM can extract robust semantic features, making it well-suited for assessing the quality and consistency of the generated novel views.

Specifically, we extract the semantic features of the i -th training view and its corresponding novel views $\mathbf{V}_i = \{f_i^j \mid j = 1, 2, \dots, M\}$. We then compute the L_2 distance between the features of the training view f_i^0 and those of each novel view f_i^j :

$$D_i = \frac{1}{M} \sum_{n=1}^M \|\mathbf{F}_{\text{DINO}}(f_i^0) - \mathbf{F}_{\text{DINO}}(f_i^n)\|_2, \quad (2)$$

where D_i is the distance between the features of the generated results and of the original image. $\mathbf{F}_{\text{DINO}}(\cdot)$ represents DINO’s feature extraction backbone, providing a global feature representation. If D_i exceeds the threshold, the novel view is too different, and we regenerate it until D_i falls below the threshold.

By applying this verification process, we expect to obtain high-quality views. Even though minor hallucinations may still remain, our GlowGS can mitigate these effects by using our novel-view semantic learning.

Feature Extraction Using high-quality views, a VFM extracts features to construct a semantic feature bank. In addition to DINO [3], other VFMs, such as CLIP [48], can be used to extract semantic features. Given a view f_i^j , the semantic features are defined as:

$$\mathbf{B}_{i,j} = \mathbf{F}_{\text{VFM}}(f_i^j), \quad (3)$$

where $\mathbf{F}_{\text{VFM}}(\cdot)$ is the feature extraction backbone of the VFM. The output, $\mathbf{B}_{i,j} = \{b_{i,j}^p \mid p = 1, 2, \dots, P\}$, represents patch-level features, where P is the number of patches, and $b_{i,j}^p$ denotes the feature of the p -th patch. The final semantic feature bank is formulated as $\mathbf{B} = \{b^s \mid s = 1, 2, \dots, S\}$, where S is the total number of patch-level features.

3.2. Novel-View Semantic Learning

During training, 3DGS models can be optimized if novel views of a scene are available with known camera poses. However, novel views generated by our image-to-video diffusion models lack camera pose information. To address this, we propose novel-view semantic learning, illustrated in the green panel in Figure 3. This process enables 3DGS

to obtain novel view information through the semantic feature bank. The key idea is that similar regions share closely related semantic features despite minor pixel-level differences. Thus, the semantic features in the bank constrain corresponding regions in novel views rendered by 3DGS. Note that our novel-view semantic learning is model-agnostic, allowing for the use of different 3DGS models.

In 3DGS, a scene is represented by a set of 3D Gaussians $\{\mathbf{G}_k(x) \mid k = 1, 2, \dots, K\}$, where K is the number of 3D Gaussians. $\mathbf{G}_k(x)$ is the k -th 3D Gaussian that can be formulated as:

$$\mathbf{G}_k(x) = e^{-\frac{1}{2}(x-\mu_k)^T \Sigma_k^{-1}(x-\mu_k)}, \quad (4)$$

where $\mu_k \in \mathbb{R}^{3 \times 1}$ and $\Sigma_k^{-1} \in \mathbb{R}^{3 \times 3}$ are the centre and covariance matrix of the k -th 3D Gaussian. Since the covariance matrices should be positive semi-definite, previous methods [26] formulate Σ_k as follows:

$$\Sigma_k = R_k S_k S_k^T R_k^T, \quad (5)$$

where S_k and R_k are the scaling matrix and rotation matrix, respectively.

The color $c(x)$ of a pixel x is built based on the spherical harmonics. It can be rendered by alpha blending, which can be expressed as:

$$c(x) = \sum_{i \in N} c_i \alpha_i \mathbf{G}_i^{2\text{D}}(x) \prod_{j=1}^{i-1} (1 - \alpha_j \mathbf{G}_j^{2\text{D}}(x)), \quad (6)$$

where N is the number of sorted 2D Gaussians associated with this pixel. $\mathbf{G}_i^{2\text{D}}$ is a 2D Gaussian transformed from the 3D Gaussian $\mathbf{G}_i(x)$. The transformation is based on a rotation matrix $\mathbf{R} \in \mathbb{R}^{3 \times 3}$ and a translation matrix $\mathbf{t} \in \mathbb{R}^{3 \times 1}$. α_i is the opacity of the 3D Gaussian $\mathbf{G}_i(x)$.

Given the rotation and translation matrix, the novel view $\bar{\mathbf{V}}$ can be rendered by Eq. 6. Note that, we do not have the ground truth of novel views. We then use a VFM $\mathbf{F}_{\text{VFM}}(\cdot)$ to extract patch-based semantic features of the novel view:

$$\bar{\mathbf{B}} = \mathbf{F}_{\text{VFM}}(\bar{\mathbf{V}}), \quad (7)$$

where $\bar{\mathbf{B}} = \{\bar{b}^p \mid p = 1, 2, \dots, P\}$ is the output of a VFM. \bar{b}^p represents the semantic features of the p -th patch.

After obtaining the semantic features of the novel view, we utilize our semantic feature bank to guide their optimization. The process consists of two steps: retrieval and semantic learning. Our retrieval process aims to search for the most similar semantic features $b^{m|p}$ in the bank \mathbf{B} for each feature \bar{b}^p . Once the most similar semantic features are found, we have paired semantic features. Our semantic learning process forces our model to reduce the distance between the paired semantic features:

$$\mathcal{L} = \lambda \mathcal{L}_{\text{ori}} + (1 - \lambda) \frac{1}{P} \sum_{p=1}^P \|\bar{b}^p - b^{m|p}\|_2, \quad (8)$$

Method	NightGlow			RawNeRF-Glow (sRGB)			Bilarf-Glow		
	PSNR \uparrow	SSIM \uparrow	LPIPS \downarrow	PSNR \uparrow	SSIM \uparrow	LPIPS \downarrow	PSNR \uparrow	SSIM \uparrow	LPIPS \downarrow
LLNeRF	25.32	0.7845	0.3029	20.75	0.5847	0.4388	18.63	0.6263	0.4033
AlethNeRF	24.94	0.7767	0.3384	23.38	0.6424	0.4250	18.19	0.5749	0.5025
3DGS	26.11	0.8156	0.2378	23.04	0.6455	0.3615	17.61	0.6171	0.3399
3DGS+Ours	27.80	0.8679	0.1869	24.39	0.6731	0.3464	18.34	0.6921	0.2799
CGS	26.20	0.8083	0.2511	23.54	0.6319	0.3712	18.12	0.6147	0.3295
CGS+Ours	27.76	0.8627	0.1902	25.29	0.6923	0.3482	18.99	0.6823	0.2766
MGS	26.46	0.8233	0.2272	23.88	0.6618	0.3492	17.76	0.6412	0.3051
MGS+Ours	28.24	0.8739	0.1847	25.37	0.7040	0.3430	19.14	0.7308	0.2404

Table 1. Comparison of performance metrics (PSNR, SSIM, and LPIPS) for methods trained on our NightGlow, RawNeRF-Glow [42], and Bilarf-Glow [54] datasets. LLNeRF [52] and AlethNeRF [11] are NeRF-based methods, while 3DGS [26], CGS [29], and MGS [64] are 3DGS-based methods. We integrate our GlowGS into three different 3DGS-based backbones for a comprehensive evaluation.

where λ is the weight that balances different losses. \mathcal{L}_{ori} is the original loss of our backbones. Since novel-view semantic learning loss does not modify 3DGS backbones, GlowGS can be applied to various 3DGS models [26, 29, 64].

4. Experiments

Since no dataset is designed for evaluating 3D scene reconstruction in nighttime glow scenes, particularly with strong glow, we introduce the NightGlow dataset. We also identify nighttime scenes with light glow effects in existing datasets, such as RawNeRF [42] and Bilarf [54], and include them for evaluation.

Our NightGlow dataset consists of 18 scenes, each with approximately 30 images. All scenes feature night glow effects, with most exhibiting strong glow. Following the settings from [26], we construct the dataset and will publicly release it. From RawNeRF-Glow [42], we select six scenes: candlefiat, gardenlights, notchbush, parkstatue, stove, and streetcorner. These scenes contain light glow effects. RawNeRF is originally designed for 3D reconstruction in the raw space, but since our method focuses on well-lit night images, particularly glow regions, we use sRGB images for our experiments. From Bilarf-Glow [54], we select three nighttime scenes: building, pondbike, and strat. Each contains light glow effects. To evaluate our method, we benchmark against three state-of-the-art (SOTA) 3D Gaussian Splatting methods [26, 29, 64] and conduct experiments on these datasets.

4.1. Implementation Details

For each scene, we use six views for training and the rest for evaluation. To ensure fair comparisons, we retain the original optimal settings of baseline methods [26, 29, 64], including the optimizer, learning rate, and other hyperparameters. We then integrate GlowGS into these backbones to enhance novel view learning. All experiments run on an A5000 GPU with 24 GB of RAM. To balance the original loss with our novel-view learning loss, we introduce a weight parameter λ , fixed at 0.01 in all experiments. GlowGS is driven by two core ideas: semantic feature generation and novel-view semantic learning.

Semantic Feature Generation In semantic feature generation, we use image-to-video diffusion models to synthesize novel views and a VFM to assess their quality. Once high-quality views are obtained, we extract their semantic features using VFMs. For our experiments, we use Pika [46] and PromeAI [47] as image-to-video diffusion models. Pika generates 3-second videos per input view, while PromeAI generates 4-second videos. We extract one frame per second, yielding three frames from Pika and four from PromeAI for each training view.

For VFM-based verification, we use DINO to measure the distance between input and generated views. If the distance exceeds 1.5, the image-to-video diffusion models regenerate novel views by adjusting the motion intensity or random seed. Once high-quality novel views are obtained, we extract robust semantic features using an VFM. We try a few models such as DINO [3], CLIP [48], and ViT [12, 15].

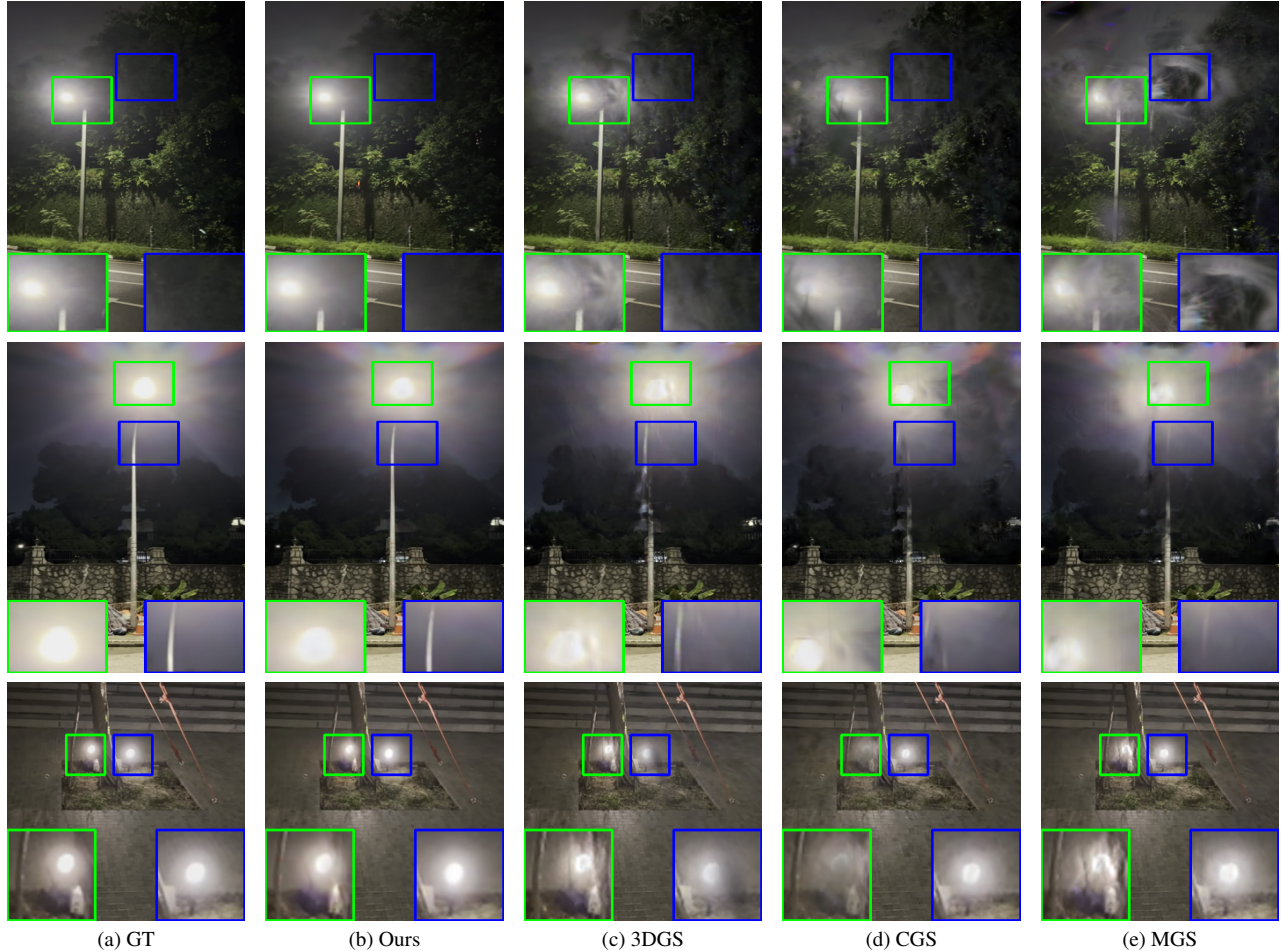


Figure 4. Qualitative results from 3DGS [26], CGS [29], MGS [64] and our method, on nighttime glow scenes. All results are from novel views. Our method not only preserves the details of night images but also effectively reconstructs glow regions. Zoom in for better visualization.

Novel-View Semantic Learning During training, we generate new camera poses by perturbing the rotation and translation matrices of the training views. After splatting, novel views are obtained. Since some VFMs support only square inputs, we randomly crop a 256×256 region from each novel view before feeding it into VFMs for semantic feature extraction. The number of patches, P , depends on the output resolution of the selected VFM.

4.2. Quantitative Evaluation

The quantitative results in Table 1 compare performance across three datasets: NightGlow, RawNeRF-Glow [42], and Bilarf-Glow [54]. While RawNeRF-Glow and Bilarf-Glow contain only light glow scenes, NightGlow includes strong glow effects. Integrating existing methods with GlowGS consistently improves performance across all datasets.

For the NightGlow dataset, we benchmark existing 3D

scene reconstruction methods, including both NeRF-based and 3DGS-based approaches. For NeRF-based methods, we select LLNeRF [52] and AlethNeRF [11], as they are designed for low-light and nighttime conditions. We also apply GlowGS to several 3D Gaussian Splatting methods, including 3DGS [26], CGS [29], and MGS [64], and compare their performance with and without novel-view semantic learning. The results, shown in Table 1, indicate that MGS achieves an average PSNR of 26.46, surpassing 3DGS and CGS by 0.35 and 0.26, respectively.

Methods with GlowGS achieve significant performance gains. MGS with GlowGS attains an average PSNR of 28.24, surpassing the original MGS by 1.78. Similarly, GlowGS improves 3DGS and CGS by 1.56 and 1.69, respectively. This improvement comes from GlowGS using image-to-video diffusion models and a VFM-based verification module to generate high-quality novel views. These views are processed by VFMs to build a semantic fea-

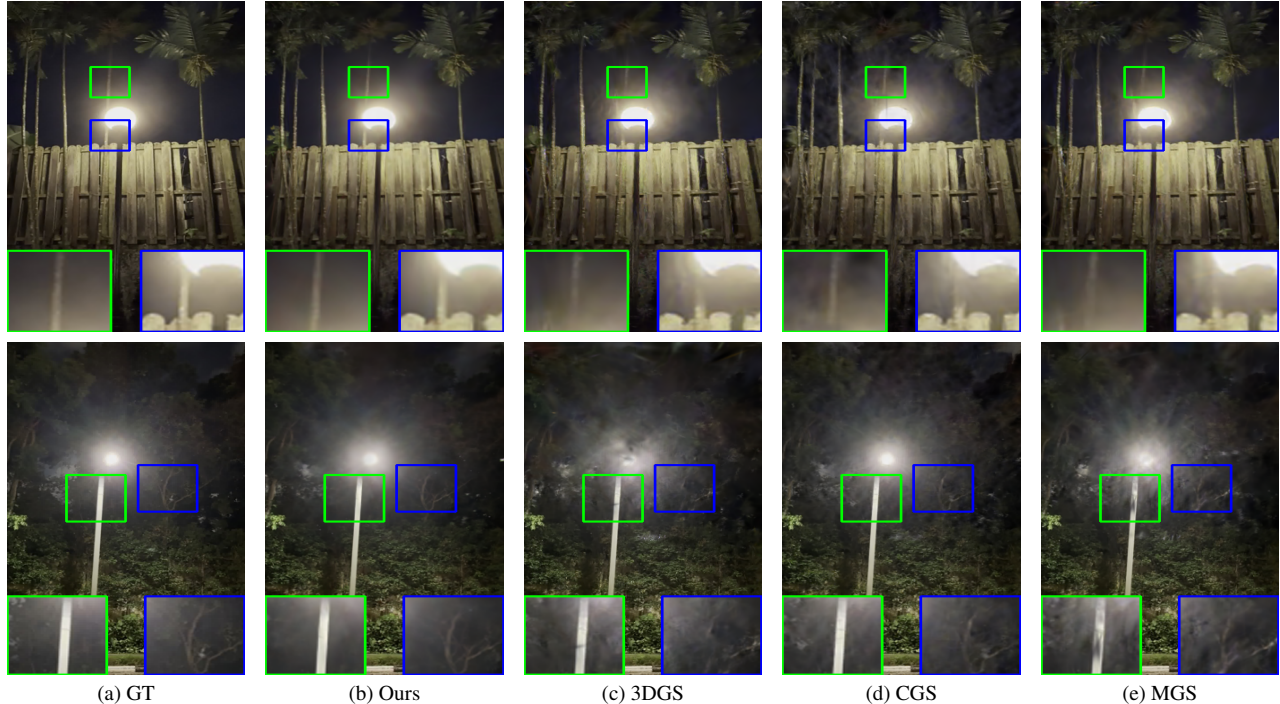


Figure 5. Qualitative results from 3DGS [26], CGS [29], MGS [64] and our method, on nighttime glow scenes. All results are from novel views. Our method not only preserves the details of night images but also effectively reconstructs glow regions. Zoom in for better visualization.

ture bank, enabling 3DGS models to optimize novel view semantics and boost performance. GlowGS consistently outperforms baseline 3DGS methods. The VFM-based verification module ensures high-quality generated views, while novel-view semantic learning enhances model training. These components work together to enable effective learning from novel views, driving superior results.

4.3. Qualitative Evaluation

Figure 4 and Figure 5 present the qualitative results of 3DGS, CGS, MGS, and our method. As shown, 3DGS, CGS, and MGS often struggle with accuracy, particularly in glow regions, where they produce floating artifacts and degrade performance. This issue arises because glow regions lack distinct structural features. While 3D Gaussians fit these regions well in training views, they fail to generalize to novel views, leading to artifacts in novel view rendering.

GlowGS uses semantic feature generation to produce high-quality novel views, rich in semantic information despite unknown camera poses. We extract robust features from these views using vision foundation models. While image-to-video diffusion models introduce some randomness, we use a VFM-based verification module to filter out major inaccuracies and hallucinations. Minor hallucinations are acceptable, as our novel-view semantic learning

enables 3DGS to selectively use valuable features for optimization. These two components significantly enhance 3DGS methods, with GlowGS successfully reconstructing glow regions, as shown in Figure 4 and Figure 5.

4.4. Ablation Studies

To evaluate the effectiveness of our semantic feature generation and novel-view semantic learning, we conducted ablation studies on the NightGlow dataset.

Analysis of Different Image-to-Video Diffusion Models

In this paper, we use image-to-video diffusion models, such as Pika [46] and PromeAI [47], to generate novel views with unknown camera poses. We conducted ablation studies with semantic feature banks generated by different diffusion models. MGS [64] serves as the baseline method, and the results are shown in Table 2. The results demonstrate that models trained with different semantic feature banks outperform the baseline. For instance, the baseline achieves a PSNR of 26.46, while models using “I2V-PIKA” and “I2V-PAI” reach PSNRs of 28.00 and 28.24, respectively, surpassing the baseline by 1.54 dB and 1.78 dB. This improvement is mainly due to our semantic feature bank, which provides rich semantic information from novel views, enabling GlowGS to effectively model nighttime scenes.

We also observe that the baseline achieves similar perfor-

I2V Diffusion Models		Vision Foundation Models			Metrics		
I2V-PIKA	I2V-PAI	ViT	CLIP	DINO	PSNR \uparrow	SSIM \uparrow	LPIPS \downarrow
					26.46	0.8233	0.2272
✓		✓			27.47	0.8657	0.1941
✓			✓		27.63	0.8696	0.2015
✓				✓	28.00	0.8724	0.1844
	✓	✓			27.34	0.8605	0.1994
	✓		✓		27.54	0.8644	0.2042
	✓			✓	28.24	0.8739	0.1847

Table 2. Comparison of performance metrics (PSNR, SSIM, and LPIPS) for methods trained on our NightGlow dataset. ‘I2V’ denotes the image-to-video diffusion models. We use ViT [12, 15], CLIP [48], and DINO [3] as vision foundation models. The first row shows the performance of the original MGS [64].

performance improvements across different image-to-video diffusion models. This is due to the VFM-based verification module, which monitors the quality of generated novel views. If a view’s score falls below expectations, it is regenerated, ensuring stable performance improvements across various generative models. During training, we first retrieve the most similar semantic features and use them to optimize novel views. This approach allows 3DGS to leverage the most effective semantic features for optimization, ensuring consistent performance gains.

Analysis of Different Vision Foundation Models In our experiments, we use various vision foundation models, including DINO [3], CLIP [48], and ViT [12, 15], to extract semantic features. To evaluate their effectiveness, we conduct ablation studies on the NightGlow dataset, using MGS [64] as the baseline. The results are presented in Table 2. The findings show that MGS, combined with different vision foundation models, significantly enhances rendering quality. For example, MGS with DINO achieves a PSNR of 28.24, surpassing the baseline by 1.78 dB. This improvement is due to GlowGS, which enables 3DGS to learn from novel views without requiring camera pose information.

We also observe that ‘‘MGS+DINO’’ achieves the highest average PSNR. For instance, ‘‘MGS+DINO’’ reaches a PSNR of 28.24, 0.9 dB higher than ‘‘MGS+ViT.’’ This is largely because DINO, trained on extensive self-supervised data, captures robust feature representations even in night glow scenes. These strong semantic features enhance the novel-view learning process, resulting in superior performance.

Analysis of Different Baselines GlowGS is a model-agnostic method, as our novel-view learning process does not require modifying the backbones of 3D Gaussian Splatting methods. To assess its effectiveness, we conduct experiments with various baselines, and the results are shown in Table 1. As expected, integrating GlowGS with 3DGS

baselines leads to substantial performance improvements. Specifically, the average PSNRs of 3DGS, CGS, and MGS are 26.11, 26.20, and 26.46, respectively. With GlowGS, these methods improve by 1.69, 1.56, and 1.78 PSNR, respectively.

This demonstrates that GlowGS enhances novel-view learning for existing 3DGS methods in nighttime scenes. As shown in Figure 4 and Figure 5, our method produces high-quality novel views. The performance gains primarily result from two key factors: semantic feature generation and novel-view semantic learning. Semantic feature generation uses image-to-video diffusion models and vision foundation models to extract features from novel views with unknown camera poses, while novel-view semantic learning optimizes these features. Together, these components drive significant performance improvements.

5. Conclusion

We introduced GlowGS, a novel nighttime 3D Gaussian Splatting method that integrates semantic feature generation and novel-view semantic learning. Our semantic feature generation synthesizes high-quality features as implicit structural cues for novel-view learning. Specifically, we use image-to-video diffusion models to generate novel views from training views, assessing their quality with a vision foundation model. We then extract semantic features from the high-quality generated views to build a semantic feature bank. Our novel-view semantic learning leverages this feature bank to optimize novel views rendered by 3DGS. For each rendered view, we extract its semantic features, search the bank for the most similar features, and minimize their distance. This allows 3DGS to compensate for missing structural cues and ensures semantically coherent, artifact-free renders. Experiments on the NightGlow dataset show that integrating GlowGS with existing 3DGS models leads to significant performance improvements.

References

- [1] Shuai Bai, Yuxuan Cai, Ruizhe Chen, Keqin Chen, Xionghui Chen, Zesen Cheng, Lianghao Deng, Wei Ding, Chang Gao, Chunjiang Ge, et al. Qwen3-vl technical report. *arXiv preprint arXiv:2511.21631*, 2025. 13
- [2] Xiao Cao, Beibei Lin, Bo Wang, Zhiyong Huang, and Robby T Tan. 3dot: Texture transfer for 3dgs objects from a single reference image. In *The Thirty-ninth Annual Conference on Neural Information Processing Systems*. 2
- [3] Mathilde Caron, Hugo Touvron, Ishan Misra, Hervé Jégou, Julien Mairal, Piotr Bojanowski, and Armand Joulin. Emerging properties in self-supervised vision transformers. In *Proceedings of the IEEE/CVF international conference on computer vision*, pages 9650–9660, 2021. 1, 2, 3, 4, 5, 8, 12
- [4] Anpei Chen, Zexiang Xu, Andreas Geiger, Jingyi Yu, and Hao Su. Tensorf: Tensorial radiance fields. In *European Conference on Computer Vision*, pages 333–350. Springer, 2022. 2
- [5] Tingting Chen, Beibei Lin, Yeying Jin, Wending Yan, Wei Ye, Yuan Yuan, and Robby T Tan. Dual-rain: Video rain removal using assertive and gentle teachers. In *European Conference on Computer Vision*, pages 127–143. Springer, 2024. 13
- [6] Tingting Chen, Srinivas Anumasa, Beibei Lin, Vedant Shah, Anirudh Goyal, and Dianbo Liu. Auto-bench: An automated benchmark for scientific discovery in llms. *arXiv preprint arXiv:2502.15224*, 2025. 13
- [7] Tingting Chen, Beibei Lin, Zifeng Yuan, Qiran Zou, Hongyu He, Anirudh Goyal, Yew-Soon Ong, and Dianbo Liu. Hypospace: Evaluating llm creativity as set-valued hypothesis generators under underdetermination. *arXiv preprint arXiv:2510.15614*, 2025. 13
- [8] Weifeng Chen, Jie Wu, Pan Xie, Hefeng Wu, Jiashi Li, Xin Xia, Xuefeng Xiao, and Liang Lin. Control-a-video: Controllable text-to-video generation with diffusion models. *arXiv preprint arXiv:2305.13840*, 2023. 3
- [9] Zhiqin Chen and Hao Zhang. Learning implicit fields for generative shape modeling. In *Proceedings of the IEEE/CVF conference on computer vision and pattern recognition*, pages 5939–5948, 2019. 2
- [10] Zhang Chen, Zhong Li, Liangchen Song, Lele Chen, Jingyi Yu, Junsong Yuan, and Yi Xu. Neurf: A neural fields representation with adaptive radial basis functions. In *Proceedings of the IEEE/CVF International Conference on Computer Vision*, pages 4182–4194, 2023. 2
- [11] Ziteng Cui, Lin Gu, Xiao Sun, Xianzheng Ma, Yu Qiao, and Tatsuya Harada. Aleth-nerf: Illumination adaptive nerf with concealing field assumption. In *Proceedings of the AAAI Conference on Artificial Intelligence*, pages 1435–1444, 2024. 5, 6
- [12] Alexey Dosovitskiy, Lucas Beyer, Alexander Kolesnikov, Dirk Weissenborn, Xiaohua Zhai, Thomas Unterthiner, Mostafa Dehghani, Matthias Minderer, Georg Heigold, Sylvain Gelly, et al. An image is worth 16x16 words: Transformers for image recognition at scale. *arXiv preprint arXiv:2010.11929*, 2020. 5, 8
- [13] Wanjun Du, Zifeng Yuan, Tingting Chen, Fucui Ke, Beibei Lin, and Shunli Zhang. Weatherreasonseg: A benchmark for weather-aware reasoning segmentation in visual language models. *arXiv preprint arXiv:2603.17680*, 2026. 13
- [14] Sara Fridovich-Keil, Alex Yu, Matthew Tancik, Qinhong Chen, Benjamin Recht, and Angjoo Kanazawa. Plenoxels: Radiance fields without neural networks. In *Proceedings of the IEEE/CVF Conference on Computer Vision and Pattern Recognition*, pages 5501–5510, 2022. 2
- [15] Stephanie Fu, Mark Hamilton, Laura Brandt, Axel Feldman, Zhoutong Zhang, and William T Freeman. Featup: A model-agnostic framework for features at any resolution. *arXiv preprint arXiv:2403.10516*, 2024. 5, 8
- [16] Yuan Gao, Guanyu Chen, Luo Qi, Wujie Fu, Zifeng Yuan, and Aaron J. Danner. Photonic ising machines for combinatorial optimization problems. *Applied Physics Reviews*, 11(4):041307, 2024. 13
- [17] Steven J Gortler, Radek Grzeszczuk, Richard Szeliski, and Michael F Cohen. The lumigraph. In *Seminal Graphics Papers: Pushing the Boundaries, Volume 2*, pages 453–464, 2023. 2
- [18] Kaiming He, Xinlei Chen, Saining Xie, Yanghao Li, Piotr Dollár, and Ross Girshick. Masked autoencoders are scalable vision learners. In *Proceedings of the IEEE/CVF conference on computer vision and pattern recognition*, pages 16000–16009, 2022. 3
- [19] Peter Hedman, Pratul P Srinivasan, Ben Mildenhall, Jonathan T Barron, and Paul Debevec. Baking neural radiance fields for real-time view synthesis. In *Proceedings of the IEEE/CVF International Conference on Computer Vision*, pages 5875–5884, 2021. 2
- [20] Jonathan Ho, Tim Salimans, Alexey Gritsenko, William Chan, Mohammad Norouzi, and David J Fleet. Video diffusion models. *Advances in Neural Information Processing Systems*, 35:8633–8646, 2022. 3
- [21] Yeying Jin, Beibei Lin, Wending Yan, Yuan Yuan, Wei Ye, and Robby T Tan. Enhancing visibility in nighttime haze images using guided apsf and gradient adaptive convolution. In *Proceedings of the 31st ACM international conference on multimedia*, pages 2446–2457, 2023. 1, 12
- [22] Fucui Ke, Zhixi Cai, Simindokht Jahangard, Weiqing Wang, Pari Delir Haghighi, and Hamid Rezatofghi. Hydra: A hyper agent for dynamic compositional visual reasoning. In *European Conference on Computer Vision*, pages 132–149. Springer, 2024. 13
- [23] Fucui Ke, Vijay Kumar B G, Xingjian Leng, Zhixi Cai, Zaid Khan, Weiqing Wang, Pari Delir Haghighi, Hamid Rezatofghi, and Manmohan Chandraker. Dwim: Towards tool-aware visual reasoning via discrepancy-aware workflow generation & instruct-masking tuning. In *Proceedings of the IEEE/CVF International Conference on Computer Vision (ICCV)*, pages 3378–3389, 2025.
- [24] Fucui Ke, Joy Hsu, Zhixi Cai, Zixian Ma, Xin Zheng, Xindi Wu, Sukai Huang, Weiqing Wang, Pari Delir Haghighi, Gholamreza Haffari, et al. Explain before you answer: A survey on compositional visual reasoning. *arXiv preprint arXiv:2508.17298*, 2025.

- [25] Fucai Ke, Zhixi Cai, Boying Li, Long Chen, Beibei Lin, Weiqing Wang, Pari Delir Haghighi, Gholamreza Haffari, and Hamid Rezatofighi. View2space: Studying multi-view visual reasoning from sparse observations. *arXiv preprint arXiv:2603.16506*, 2026. [13](#)
- [26] Bernhard Kerbl, Georgios Kopanas, Thomas Leimkühler, and George Drettakis. 3d gaussian splatting for real-time radiance field rendering. *ACM Transactions on Graphics*, 42(4):1–14, 2023. [1](#), [2](#), [4](#), [5](#), [6](#), [7](#)
- [27] Alexander Kirillov, Eric Mintun, Nikhila Ravi, Hanzi Mao, Chloe Rolland, Laura Gustafson, Tete Xiao, Spencer Whitehead, Alexander C Berg, Wan-Yen Lo, et al. Segment anything. In *Proceedings of the IEEE/CVF International Conference on Computer Vision*, pages 4015–4026, 2023. [3](#)
- [28] Jonas Kulhanek and Torsten Sattler. Tetra-nerf: Representing neural radiance fields using tetrahedra. In *Proceedings of the IEEE/CVF International Conference on Computer Vision*, pages 18458–18469, 2023. [2](#)
- [29] Joo Chan Lee, Daniel Rho, Xiangyu Sun, Jong Hwan Ko, and Eunbyung Park. Compact 3d gaussian representation for radiance field. *Proceedings of the IEEE/CVF Conference on Computer Vision and Pattern Recognition*, 2024. [1](#), [2](#), [5](#), [6](#), [7](#)
- [30] Marc Levoy and Pat Hanrahan. Light field rendering. In *Seminal Graphics Papers: Pushing the Boundaries, Volume 2*, pages 441–452. 2023. [2](#)
- [31] Shuwei Li and Robby T Tan. Nightcc: nighttime color constancy via adaptive channel masking. In *Proceedings of the IEEE/CVF Conference on Computer Vision and Pattern Recognition*, pages 25522–25531, 2024. [13](#)
- [32] Shuwei Li, Lei Tan, and Robby T Tan. Bridging day and night: Target-class hallucination suppression in unpaired image translation. In *Proceedings of the AAAI Conference on Artificial Intelligence*, pages 6424–6432, 2026. [13](#)
- [33] Beibei Lin, Tingting Chen, and Robby T Tan. Geocomplete: Geometry-aware diffusion for reference-driven image completion. In *The Thirty-ninth Annual Conference on Neural Information Processing Systems*, . [3](#)
- [34] Beibei Lin, Zifeng Yuan, and Tingting Chen. Rgb-to-polarization estimation: A new task and benchmark study. In *The Thirty-ninth Annual Conference on Neural Information Processing Systems Datasets and Benchmarks Track*, .
- [35] Beibei Lin, Yeying Jin, Wending Yan, Wei Ye, Yuan Yuan, Shunli Zhang, and Robby T Tan. Nightrain: Nighttime video deraining via adaptive-rain-removal and adaptive-correction. In *Proceedings of the AAAI Conference on Artificial Intelligence*, pages 3378–3385, 2024. [3](#)
- [36] Beibei Lin, Yeying Jin, Yan Wending, Wei Ye, Yuan Yuan, and Robby T Tan. Nighthaze: Nighttime image dehazing via self-prior learning. In *Proceedings of the AAAI Conference on Artificial Intelligence*, pages 5209–5217, 2025. [1](#)
- [37] Beibei Lin, Stephen Lin, and Robby Tan. Seeing beyond haze: Generative nighttime image dehazing. *arXiv preprint arXiv:2503.08073*, 2025. [3](#)
- [38] Nelson Max. Optical models for direct volume rendering. *IEEE Transactions on Visualization and Computer Graphics*, 1(2):99–108, 1995. [2](#)
- [39] Nelson Max and Min Chen. Local and global illumination in the volume rendering integral. Technical report, Lawrence Livermore National Lab.(LLNL), Livermore, CA (United States), 2005. [2](#)
- [40] Lars Mescheder, Michael Oechsle, Michael Niemeyer, Sebastian Nowozin, and Andreas Geiger. Occupancy networks: Learning 3d reconstruction in function space. In *Proceedings of the IEEE/CVF conference on computer vision and pattern recognition*, pages 4460–4470, 2019. [2](#)
- [41] Ben Mildenhall, Pratul P Srinivasan, Matthew Tancik, Jonathan T Barron, Ravi Ramamoorthi, and Ren Ng. Nerf: Representing scenes as neural radiance fields for view synthesis. *Communications of the ACM*, 65(1):99–106, 2021. [2](#)
- [42] Ben Mildenhall, Peter Hedman, Ricardo Martin-Brualla, Pratul P Srinivasan, and Jonathan T Barron. Nerf in the dark: High dynamic range view synthesis from noisy raw images. In *Proceedings of the IEEE/CVF conference on computer vision and pattern recognition*, pages 16190–16199, 2022. [5](#), [6](#), [13](#)
- [43] Thomas Müller, Alex Evans, Christoph Schied, and Alexander Keller. Instant neural graphics primitives with a multiresolution hash encoding. *ACM transactions on graphics (TOG)*, 41(4):1–15, 2022. [2](#)
- [44] Jeong Joon Park, Peter Florence, Julian Straub, Richard Newcombe, and Steven Lovegrove. DeepSDF: Learning continuous signed distance functions for shape representation. In *Proceedings of the IEEE/CVF conference on computer vision and pattern recognition*, pages 165–174, 2019. [2](#)
- [45] William Peebles and Saining Xie. Scalable diffusion models with transformers. In *Proceedings of the IEEE/CVF International Conference on Computer Vision*, pages 4195–4205, 2023. [3](#)
- [46] Pika. Pika: Ai video creation platform, 2024. [1](#), [3](#), [5](#), [7](#), [12](#)
- [47] PromeAI. Promeai: Professional ai solutions, 2024. [1](#), [3](#), [5](#), [7](#), [12](#)
- [48] Alec Radford, Jong Wook Kim, Chris Hallacy, Aditya Ramesh, Gabriel Goh, Sandhini Agarwal, Girish Sastry, Amanda Askell, Pamela Mishkin, Jack Clark, et al. Learning transferable visual models from natural language supervision. In *International conference on machine learning*, pages 8748–8763. PMLR, 2021. [1](#), [2](#), [3](#), [4](#), [5](#), [8](#), [12](#)
- [49] Christian Reiser, Songyou Peng, Yiyi Liao, and Andreas Geiger. Kilonerf: Speeding up neural radiance fields with thousands of tiny mlps. In *Proceedings of the IEEE/CVF international conference on computer vision*, pages 14335–14345, 2021. [2](#)
- [50] Robin Rombach, Andreas Blattmann, Dominik Lorenz, Patrick Esser, and Björn Ommer. High-resolution image synthesis with latent diffusion models. In *Proceedings of the IEEE/CVF conference on computer vision and pattern recognition*, pages 10684–10695, 2022. [3](#)
- [51] Zhiqiang Teng, Beibei Lin, Tingting Chen, Zifeng Yuan, Xuanyi Li, Xuanyu Zhang, and Shunli Zhang. Raindropgs: A benchmark for 3d gaussian splatting under raindrop conditions. *arXiv preprint arXiv:2510.17719*, 2025. [2](#)
- [52] Haoyuan Wang, Xiaogang Xu, Ke Xu, and Rynson WH Lau. Lighting up nerf via unsupervised decomposition and enhancement. In *Proceedings of the IEEE/CVF International*

- Conference on Computer Vision*, pages 12632–12641, 2023. [5](#), [6](#)
- [53] Yaohui Wang, Piotr Bilinski, Francois Bremond, and Antitza Dantcheva. Imaginator: Conditional spatio-temporal gan for video generation. In *Proceedings of the IEEE/CVF Winter Conference on Applications of Computer Vision*, pages 1160–1169, 2020. [3](#)
- [54] Yuehao Wang, Chaoyi Wang, Bingchen Gong, and Tianfan Xue. Bilateral guided radiance field processing. *ACM Transactions on Graphics (TOG)*, 43(4):1–13, 2024. [5](#), [6](#), [13](#)
- [55] Jay Zhangjie Wu, Yixiao Ge, Xintao Wang, Stan Weixian Lei, Yuchao Gu, Yufei Shi, Wynne Hsu, Ying Shan, Xiaohu Qie, and Mike Zheng Shou. Tune-a-video: One-shot tuning of image diffusion models for text-to-video generation. In *Proceedings of the IEEE/CVF International Conference on Computer Vision*, pages 7623–7633, 2023. [3](#)
- [56] Qiangeng Xu, Zexiang Xu, Julien Philip, Sai Bi, Zhixin Shu, Kalyan Sunkavalli, and Ulrich Neumann. Pointerf: Point-based neural radiance fields. In *Proceedings of the IEEE/CVF conference on computer vision and pattern recognition*, pages 5438–5448, 2022. [2](#)
- [57] Weilong Yan, Robby T. Tan, Bing Zeng, and Shuaicheng Liu. Deep homography mixture for single image rolling shutter correction. In *Proceedings of the IEEE/CVF International Conference on Computer Vision (ICCV)*, pages 9868–9877, 2023. [13](#)
- [58] Weilong Yan, Ming Li, Haipeng Li, Shuwei Shao, and Robby T. Tan. Synthetic-to-real self-supervised robust depth estimation via learning with motion and structure priors. In *Proceedings of the Computer Vision and Pattern Recognition Conference (CVPR)*, pages 21880–21890, 2025. [13](#)
- [59] Weilong Yan, Xin Zhang, and Robby T Tan. Er-lora: Effective-rank guided adaptation for weather-generalized depth estimation. *arXiv preprint arXiv:2509.00665*, 2025. [13](#)
- [60] Weilong Yan, Haipeng Li, Hao Xu, Nianjin Ye, Yihao Ai, Shuaicheng Liu, and Jingyu Hu. LaS-Comp: Zero-shot 3D Completion with Latent-Spatial Consistency. *arXiv preprint arXiv:2602.18735*, 2026. [13](#)
- [61] Xin Yang, Xin Zhang, and Xinchao Wang. Erf: A benchmark dataset for robust semantic segmentation under extreme rainfall conditions. In *Proceedings of the AAAI Conference on Artificial Intelligence*, pages 9301–9309, 2025. [13](#)
- [62] Lior Yariv, Peter Hedman, Christian Reiser, Dor Verbin, Pratul P Srinivasan, Richard Szeliski, Jonathan T Barron, and Ben Mildenhall. Baked sdf: Meshing neural sdf for real-time view synthesis. In *ACM SIGGRAPH 2023 Conference Proceedings*, pages 1–9, 2023. [2](#)
- [63] Alex Yu, Ruilong Li, Matthew Tancik, Hao Li, Ren Ng, and Angjoo Kanazawa. Plenotrees for real-time rendering of neural radiance fields. In *Proceedings of the IEEE/CVF International Conference on Computer Vision*, pages 5752–5761, 2021. [2](#)
- [64] Zehao Yu, Anpei Chen, Binbin Huang, Torsten Sattler, and Andreas Geiger. Mip-splatting: Alias-free 3d gaussian splatting. *Proceedings of the IEEE/CVF Conference on Computer Vision and Pattern Recognition*, 2024. [1](#), [2](#), [3](#), [5](#), [6](#), [7](#), [8](#), [12](#), [13](#)
- [65] Zifeng Yuan, Tingting Chen, Dewen Zhang, Yuan Gao, Wenkai Shan, Beibei Lin, and Aaron J. Danner. Tailored polarization-switchable VCSEL arrays for photonic ising computing. *Applied Physics Letters*, 127(22):221102, 2025. [13](#)
- [66] Zifeng Yuan, Wenkai Shan, Tingting Chen, Beibei Lin, and Aaron J. Danner. Mesa orientation engineering for polarization locking in VCSELs. In *2025 IEEE Photonics Conference (IPC)*, pages 1–2, Singapore, Singapore, 2025. [13](#)
- [67] Zifeng Yuan, Dewen Zhang, Yuan Gao, Luo Qi, Wujie Fu, and Aaron J. Danner. Large-scale fabrication and analysis of polarization behavior in VCSELs with tailored apertures. *Journal of Lightwave Technology*, 43(14):6819–6827, 2025.
- [68] Zifeng Yuan, Dewen Zhang, Hong-Lin Lin, and Aaron J. Danner. Engineering polarization switching in VCSELs with custom aperture shapes. In *CLEO: Conference on Lasers and Electro-Optics*, page JPS200.47. Optica Publishing Group, 2025. [13](#)
- [69] Zifeng Yuan, Dewen Zhang, Lei Shi, Yutong Liu, and Aaron J. Danner. Enhanced polarization locking in VCSELs. *Applied Physics Letters*, 126(15):151101, 2025. [13](#)
- [70] Dewen Zhang, Zifeng Yuan, Thanh Xuan Hoang, Wujie Fu, Ching Eng Png, Soon Thor Lim, and Aaron J. Danner. All-optical scalable and programmable VCSEL-based ising annealer with parallel feedback. *Optics Express*, 33(11):22119–22131, 2025. [13](#)
- [71] Xin Zhang and Robby T Tan. Mamba as a bridge: Where vision foundation models meet vision language models for domain-generalized semantic segmentation. In *Proceedings of the IEEE/CVF Conference on Computer Vision and Pattern Recognition*, pages 14527–14537, 2025. [13](#)
- [72] Xin Zhang, Jinheng Xie, Yuan Yuan, Michael Bi Mi, and Robby T Tan. Heap: unsupervised object discovery and localization with contrastive grouping. In *Proceedings of the AAAI Conference on Artificial Intelligence*, pages 7323–7331, 2024. [13](#)

Table 3. (PSNR/SSIM) vs. Number of Training Views

Method	2 views	4 views	6 views	8 views	10 views
MGS [64]	21.0/0.64	25.8/0.80	26.5/0.82	27.6/0.84	28.2/0.85
MGS [64] + Ours	22.1/0.72	27.2/0.85	28.2/0.87	29.2/0.88	29.8/0.90

A. Visualization

This paper harnesses vision foundation models to help the reconstruction of nighttime glow scenes. The motivation is that VFMs can generate discriminative representations in glow regions. We show more visualization results in Figure 6.

B. Experimental Details

In this paper, we leverage image-to-video diffusion models and vision foundation models (VFMs) to enable our 3DGS framework to effectively reconstruct nighttime glow scenes. Given a training view, we first use image-to-video diffusion models to generate novel views with unknown camera poses. A VFM-based verification module then assesses the quality of these novel views. Once the high-quality generated views are obtained, we extract robust semantic features using VFMs to construct a semantic feature bank. The experimental details are as follows:

Image-to-Video Diffusion Models We employ state-of-the-art image-to-video diffusion models, such as Pika [46] and PromeAI [47], to synthesize novel views. Pika and PromeAI generate 3-second and 4-second videos per input view, respectively. We then extract one frame per second, resulting in three frames from Pika and four from PromeAI for each training view. For Pika, we do not use a text prompt to guide the generation process, whereas for PromeAI, we use the prompt: “Slow camera movement, static scene, no new objects.”

VFM-Based Verification We use DINO to measure the distance between the input and generated views, as shown in Figure 8. If the distance exceeds 1.5, the image-to-video diffusion models re-generate novel views by adjusting the motion intensity or random seed. Specifically, for PromeAI, both motion intensity and the random seed can be adjusted, whereas for Pika, only the random seed can be modified.

Feature Extraction We leverage vision foundation models such as DINO [3] and CLIP [48] to extract semantic features, which are then stored in a semantic feature bank.

C. Evaluation on Glow and Non-Glow Regions

Glow is defined as the area surrounding a light source where luminance gradually decays but remains above a certain

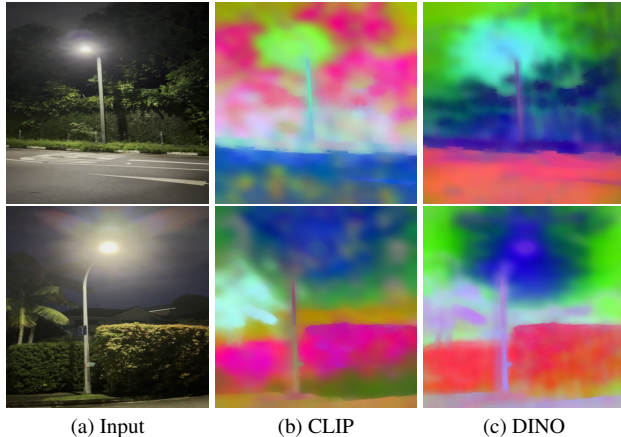


Figure 6. Visualization of features extracted by different Vision Foundation Models.

threshold (e.g., 10% of the source peak). In practice, this region can be approximated using an Atmospheric Point Spread Function (APSF) [21] centered on the detected light source. Fig. 7 illustrates the resulting glow mask. Based on the generated glow mask, PSNR and SSIM are computed separately for the glow and non-glow regions. Table 4 shows that our method achieves significant improvements in both regions.

D. Ablation Studies

In this section, we present additional ablation studies to verify the effectiveness of GlowGS.

Analysis of the Number of Training Views In our experimental setup, each scene includes six training views, with the remaining frames used for evaluation. To assess the robustness of GlowGS, we perform ablation studies with varying numbers of training views. As shown in Table 3, our method consistently outperforms baseline approaches, regardless of the number of training views. This improvement stems from our novel-view semantic learning strategy, which optimizes rendered novel views without requiring ground-truth supervision.

Analysis of Generated Views The additional generated views total 18 for Pika and 24 for PromeAI. To assess the impact of the number of generated views, we conduct experiments using 0, 12, and 24 additional views. Our method achieves PSNR/SSIM scores of 26.46/0.8233, 27.53/0.8650, and 28.24/0.8739 for 0, 12, and 24 additional views, respectively. These results indicate that increasing the number of generated views improves performance. Note that these images cannot directly train 3DGS due to unknown camera poses.

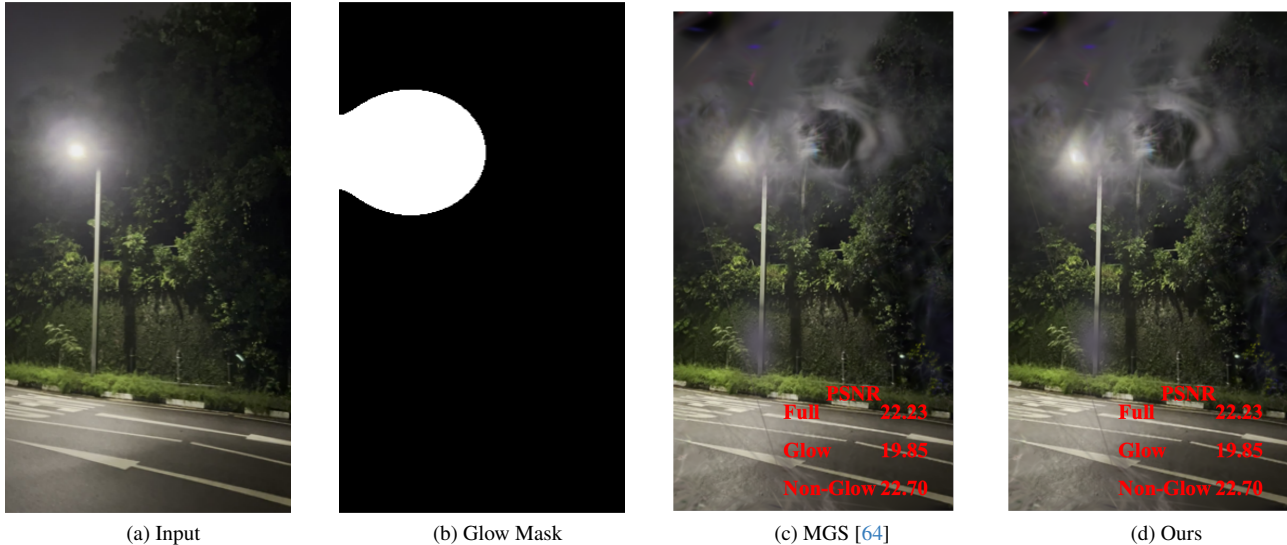


Figure 7. Glow masks and results from MGS [64] and ours.

Table 4. (PSNR \uparrow / SSIM \uparrow / LPIPS \downarrow) computed separately on glow and non-glow regions using the glow mask.

Method	NightGlow		RawNerf-Glow (sRGB) [42]		Bilarf-Glow [54]	
	Glow Regions	Non-Glow Regions	Glow Regions	Non-Glow Regions	Glow Regions	Non-Glow Regions
MGS [64]	25.7 / 0.97 / 0.2154	26.9 / 0.84 / 0.2298	18.4 / 0.97 / 0.3723	24.7 / 0.67 / 0.3491	17.8 / 0.93 / 0.2853	18.1 / 0.69 / 0.3098
MGS [64]+ours	28.1 / 0.98 / 0.1610	28.6 / 0.89 / 0.1893	22.0 / 0.98 / 0.3189	26.0 / 0.71 / 0.3446	18.4 / 0.94 / 0.2292	19.9 / 0.78 / 0.2418

E. Future Directions

Future work may further enhance GlowGS by incorporating Vision-Language Models (VLMs) [1] and stronger Vision Foundation Models (VFMs) for robust semantic segmentation and depth estimation in adverse weather [58, 59, 61, 71, 72], visual reasoning [6, 7, 13, 22–25], geometric completion/correction [57, 60], and scene enhancement [5, 31, 32]. In addition, integrating richer modalities, such as segmentation priors, polarization cues [66–68], and physics-based computational imaging constraints [16, 65, 69, 70], could provide complementary structural and physical information for more robust nighttime glow reconstruction and novel-view synthesis.

F. Ethical Considerations

This paper introduces a new nighttime glow dataset, comprising 18 scenes. Each scene contains approximately 30 images, all affected by glow effects. To ensure privacy and ethical compliance, our collected images do not include any identifiable individuals, vehicles, or sensitive content. Additionally, our dataset is intended solely for research purposes, focusing on improving nighttime scene reconstruction without infringing on personal privacy or security concerns. We adhere to ethical data collection guidelines and

ensure that no copyrighted or restricted content is included in our dataset.



Figure 8. Visualization of generated results. Given a training view, we use image-to-video diffusion models to synthesize novel views. The last three columns show the outputs of these models. Red bounding boxes highlight high-quality results below the threshold, while blue bounding boxes indicate low-quality results exceeding the threshold.